BIOCELL

Tech Science Press

http://doi.org/10.32604/biocell.2026.076364

ARTICLE

12-O-Tetradecanoylphorbol-13-Acetate Inhibits TGF-β1-Induced Proliferation and Fibrosis in LX-2 Hepatic Stellate Cells by Regulating both YAP and AKT Activities

Moo Hyun Kim[1], Yongdae Yoon[2], Chang Wan Kim[1], Jun-Won Lee[3], Bhupendra Regmi[2], Saher Fatima[2], Moon Young Kim[2,3], Soon Koo Baik[2,3], Pil Young Jung[1,*] and Young Woo Eom[2,*]

[1]Department of Surgery, Yonsei University Wonju College of Medicine, Wonju, Republic of Korea
[2]Regeneration Medicine Research Center, Yonsei University Wonju College of Medicine, Wonju, Republic of Korea
[3]Department of Internal Medicine, Yonsei University Wonju College of Medicine, Wonju, Republic of Korea
*Corresponding Authors: Pil Young Jung. Email: surgery4trauma@yonsei.ac.kr; Young Woo Eom. Email: yweom@yonsei.ac.kr

Received: 19 November 2025; Accepted: 04 March 2026; Published: 09 June 2026

ABSTRACT: Background: Although transforming growth factor-β (TGF-β) drives hepatic stellate cell activation and fibrogenesis, the mechanisms by which 12-O-tetradecanoylphorbol-13-acetate (TPA) modulates these processes in TGF-β1-activated hepatic stellate cells remain to be determined. Therefore, we investigated whether TPA alleviates fibrosis in TGF-β1-treated hepatic stellate cells and regulates both canonical and non-canonical pathways. Further, we assessed whether inhibitors of these pathways similarly affect proliferation and fibrosis in LX-2 cells. **Methods:** LX-2 hepatic stellate cells were used as the experimental model. Cells were treated with TPA, TGF-β, or TGF-β plus TPA, and Yes-associated protein (YAP) and protein kinase B (PKB; AKT) phosphorylation, as well as YAP intracellular localization, were assessed. PKC-δ involvement was examined using the pan-PKC inhibitor Go 6983, and the roles of YAP and AKT in TGF-β1-activated LX-2 cells were evaluated using verteporfin and AKTI-1/2, respectively. **Results:** TPA significantly increased YAP phosphorylation and reduced its nuclear translocation, resulting in decreased LX-2 cell proliferation and fibronectin (FN1) production. Although TPA also inhibited AKT phosphorylation, FN1 expression was primarily regulated by YAP inhibition. Notably, proliferation in TGF-β1-treated LX-2 cells was suppressed only upon co-administration of both inhibitors. Our results suggest that coordinated regulation of YAP and AKT activity is essential for controlling fibroblast proliferation and ECM production. **Conclusions:** These findings suggest that in TGF-β-activated hepatic stellate cells, YAP simultaneously controls proliferation and fibrosis, and AKT regulates only proliferation. Therefore, TPA, which regulates both YAP and AKT activity, may be a promising therapeutic candidate for liver fibrosis treatment by simultaneously controlling proliferation and fibrosis in hepatic stellate cells.

KEYWORDS: 12-O-tetradecanoylphorbol-13-acetate; yes-associated protein; protein kinase B; hepatic stellate cell; transforming growth factor-β1

1 Introduction

The transforming growth factor-β (TGF-β) signaling pathway regulates cell proliferation, migration, differentiation, and apoptosis to maintain tissue and organ homeostasis [1–3]. In fibrotic diseases, TGF-β induces fibroblast differentiation into myofibroblasts and promotes excessive extracellular matrix (ECM) accumulation [4,5]. In liver disease, TGF-β is a key regulator of hepatic stellate cell activation and ECM deposition, making it the most physiologically relevant inducer of liver fibrosis [6,7]. Therefore, TGF-β-related research is essential for accurately studying the mechanisms of fibrosis and evaluating

anti-fibrotic therapeutic strategies. TGF-β signaling consists of both canonical and non-canonical pathways [8,9]. The canonical pathway involves receptor-regulated, common mediator, and inhibitory SMA and MAD-related proteins (SMADs; R-, Co-, and I-SMAD, respectively). Upon ligand binding, TGF-β associates with single transmembrane type I and II receptors (TβRI and TβRII) and induces R-SMADs (SMAD2 and SMAD3) phosphorylation. Phosphorylated R-SMADs form a trimeric complex with SMAD4 (Co-SMAD), translocate into the nucleus, and induce TGF-β-responsive gene expression, such as α-smooth muscle actin (α-SMA), collagens (COLs), and fibronectin (FN1) [10–12]. In the non-canonical pathway, TGF-β mediates biological responses and regulates the canonical SMAD pathway through Rho GTPases (Rho), mitogen-activated protein kinases (MAPK), and phosphoinositide-3-kinase (PI3K)/protein kinase B (PKB or AKT) [8,13].

The Hippo signaling pathway is associated with the pathophysiology of fibrotic diseases in many organs, including the lung [14,15], heart [16,17], liver [18,19], kidney [20,21], and skin [22,23]. Yes-associated protein (YAP) and transcriptional coactivator with PDZ-binding motif (TAZ) function as central downstream effectors of the Hippo signaling. In the inactive state of Hippo signaling, unphosphorylated YAP/TAZ translocate into the nucleus and bind to TEA domain (TEAD) DNA-binding proteins, leading to the expression of target genes such as CTGF, CYR61, and MYC [24–26]. Extracellular ligands, organ size, mechanotransduction, environmental stress, energy stress, and cell–cell contact can activate the Hippo pathway through a kinase signaling cascade involving MST1/2, LATS1/2, SAV1, MOB1, and YAP [26–28]. Phosphorylated YAP undergoes proteolytic degradation in the cytoplasm after its nuclear translocation is blocked, thereby halting target gene expression [27,29,30]. Moreover, the Hippo pathway cooperates with the canonical SMAD pathway to co-regulate the expression of TGF-β-responsive genes, including α-SMA, FN1, COL1A1, COL4A1, CTGF, and CYR61 [31,32].

We previously reported that 12-O-tetradecanoylphorbol-13-acetate (TPA), a protein kinase C (PKC) activator, promotes YAP phosphorylation and thereby inhibits fibrosis in LX-2 hepatic stellate cells (LX-2) [33]. However, despite the potential of TPA to regulate YAP or AKT activity, only a few studies have demonstrated that TPA controls fibrosis. Furthermore, to the best of our knowledge, no reports indicate whether TPA can regulate hepatic stellate cell proliferation and fibrosis by modulating YAP and AKT activity in TGF-β-induced fibrotic responses. AKT is a mediator of the non-canonical TGF-β pathway and regulates the activity of hepatic stellate cells [34–36]. Additionally, TPA reportedly regulates AKT phosphorylation [37–39]. These findings suggest that TPA could simultaneously regulate both the canonical and non-canonical TGF-β pathways through modulation of YAP and AKT. Here, we investigated whether TPA alleviates fibrosis in TGF-β1-treated hepatic stellate cells and regulates both canonical and non-canonical pathways. Further, we assessed whether inhibitors of these pathways similarly affect proliferation and fibrosis in LX-2 cells.

2 Materials and Methods

2.1 Reagents

TPA (P8139), methylthiazolyldiphenyl-tetrazolium bromide (MTT, M2128), and verteporfin (VP, SML0534) were purchased from Sigma-Aldrich (St. Louis, MO, USA). Go 6983 (HY-13689), a pan-PKC inhibitor, was purchased from MedChemExpress (Princeton, NJ, USA). AKTI-1/2 (S7776), an AKT inhibitor, was acquired from Selleck Chemicals (Houston, TX, USA). Recombinant human TGF-β1 was supplied by R&D Systems (Minneapolis, MN, USA).

For immunoblotting analyses, antibodies against GAPDH (sc-47724, 1:1000), PKC-δ (sc-396, 1:1000), and YAP (sc-101199, 1:1000) were obtained from Santa Cruz Biotechnology (Dallas, TX, USA). Antibodies specific

for AKT (#9272, 1:2000), phosphorylated AKT (#4060, 1:2000), COL1A1 (#39952, 1:2000), phosphorylated YAP (#4911, 1:2000), phosphorylated-PKC-δ (#9374, 1:2000), as well as horseradish peroxidase-conjugated secondary antibodies (#7074 or #7076, 1:2000), were purchased from Cell Signaling Technology (Danvers, MA, USA). The FN1 antibody (F6140, 1:2000) was obtained from Sigma-Aldrich, and the α-smooth muscle actin (α-SMA) antibody (ab5694, 1:2000) was procured from Abcam (Cambridge, UK). All remaining chemicals and reagents were purchased from Sigma-Aldrich unless otherwise stated.

2.2 Cell Culture

LX-2 cells (Millipore, Burlington, MA, USA) were cultured in high-glucose Dulbecco's Modified Eagle Medium (DMEM; Gibco, Thermo Fisher Scientific, Waltham, MA, USA) containing 3% fetal bovine serum (FBS; Gibco, Thermo Fisher Scientific) and penicillin-streptomycin (Gibco, Thermo Fisher Scientific). Cells were incubated at 37°C under a humidified atmosphere containing 5% CO_2. LX-2 cells were periodically tested for mycoplasma contamination using a mycoplasma detection kit (MP Biomedicals, 093050201, Irvine, CA, USA), and no contamination was observed during the study. For experimental procedures, cells were plated and allowed to adhere for 24 h before stimulation. TGF-β1 (1 ng/mL) or TPA (10 nM) was then administered for either 3 h or 48 h, depending on the experimental requirement. When indicated, Go 6983, VP, or AKTI-1/2 was added 20 min before TGF-β1 treatment. As previously described [33], we used TGF-β1 (1 ng/mL) and TPA (10 nM) at a single concentration.

2.3 MTT Assay

LX-2 cells were plated in 96-well culture plates at a density of 1×10^4 cells/cm^2 and allowed to stabilize for 24 h. Cells were subsequently exposed to TGF-β1 (1 ng/mL) alone, TPA (10 nM) alone, or TGF-β1 + TPA for an additional 48 h. Where indicated, Go 6983 (1 μM), VP (025–2.5 μM), or AKTI-1/2 (0.01–0.5 μM) was administered 20 min before the addition of TGF-β1 to inhibit components of the TGF-β signaling cascade. After treatment, MTT prepared in phosphate-buffered saline (PBS, pH 7.4) was added to each well to achieve a final concentration of 5 mg/mL, followed by incubation at 37°C for 2 h. The resulting formazan products were solubilized in 100 μL of dimethyl sulfoxide, and absorbance was recorded at 570 nm using a microplate reader (SpectraMax 190; Molecular Devices, San Jose, CA, USA).

2.4 Immunoblotting

Protein expression was examined using standard immunoblotting methods. LX-2 cells were lysed using RIPA buffer (89900, Thermo Fisher Scientific) supplemented with protease and phosphatase inhibitor cocktails (P3100, GenDEPOT, Katy, TX, USA), and total protein concentrations were quantified using a colorimetric protein assay kit (#500-0006, Bio-Rad Laboratories, Hercules, CA, USA). Equivalent amounts of protein (30 μg) were separated using 10% sodium dodecyl sulfate-polyacrylamide gel electrophoresis and transferred onto PVDF membranes (Immobilon-P; IPVH00010, Millipore). Membranes were blocked with 5% skim milk dissolved in Tris-buffered saline containing 0.05% Tween 20 (TBST; 50 mM Tris-HCl, pH 7.6; 150 mM NaCl) and incubated overnight at 4°C with primary antibodies against α-SMA, FN1, COL1A1, p-AKT, AKT, p-YAP, YAP, and GAPDH. After three TBST washes (5 min each), membranes were incubated with horseradish peroxidase-conjugated secondary antibodies for 1 h at room temperature. Signals were visualized using the EZ-Western Lumi Pico (DG-WP500, Dogen, Seoul, Republic of Korea) or Femto detection reagents (DG-WF200, Dogen) and captured using a ChemiDoc XRS+ imaging system (Bio-Rad). Band intensities were quantified using ImageJ software (version 1.52a; NIH, Bethesda, MD, USA). The half maximal inhibitory concentration (IC_{50}) was determined by treating cells with increasing concentrations

of AKTI-1/2 or VP and quantifying the corresponding band intensities of p-AKT or CYR61, respectively, followed by nonlinear regression analysis.

2.5 Immunocytochemical Analysis

For visualization of YAP subcellular localization, LX-2 cells were cultured on glass coverslips and treated with TGF-β1 (1 ng/mL) and/or TPA (10 nM) for 3 h. Cells were rinsed with PBS (pH 7.4), fixed in 4% paraformaldehyde, permeabilized with 0.2% Triton X-100 for 10 min at 25°C, and then blocked for 30 min in PBS containing 3% FBS. Samples were incubated overnight at 4°C with a YAP primary antibody (1:100; sc-101199, Santa Cruz Biotechnology). An Alexa Fluor 488 conjugated secondary antibody (1:100; A28175, Invitrogen, Carlsbad, CA, USA) was applied for 1 h at 25°C to visualize staining. Following washing, coverslips were mounted with ProLong™ Gold Antifade Mountant (Invitrogen) containing 4′,6-diamidino-2-phenylindole (DAPI). Images were captured using an Eclipse TS2R fluorescence microscope (Nikon, Tokyo, Japan). Nuclear YAP intensity was quantified by densitometry using ImageJ.

2.6 Statistical Analysis

Results are presented as the mean ± standard deviation. Statistical comparisons between groups were performed using Student's *t*-test or one-way analysis of variance (ANOVA) with Scheffé's post hoc test. Differences were considered statistically significant when $p < 0.05$.

3 Results

3.1 Effects of TPA on TGF-β1-Induced Proliferation and Fibrosis in LX-2 Cells

Previously, we observed that TPA increases YAP phosphorylation, thereby reducing α-SMA expression in LX-2 cells [33]. YAP can cooperate with TGF-β-dependent SMAD signaling to regulate fibrosis; therefore, we investigated whether TPA modulates proliferation and fibrosis in TGF-β1-treated LX-2 cells. TGF-β1 increased the growth rate and expression of fibrosis-related proteins, including α-SMA, FN1, and COL1A1, in LX-2 cells. However, TPA significantly reduced TGF-β1-induced proliferation (from 115.20 ± 5.09 to 77.45 ± 4.10) and α-SMA, FN1, and COL1A1 expression (Fig. 1). In LX-2 cells, TGF-β-induced expression of α-SMA, FN1, and COL1A1 exhibited largely similar patterns; therefore, FN1 was used as a representative fibrosis marker in this study. These results suggest that TPA can effectively regulate TGF-β1-induced activation of hepatic stellate cells.

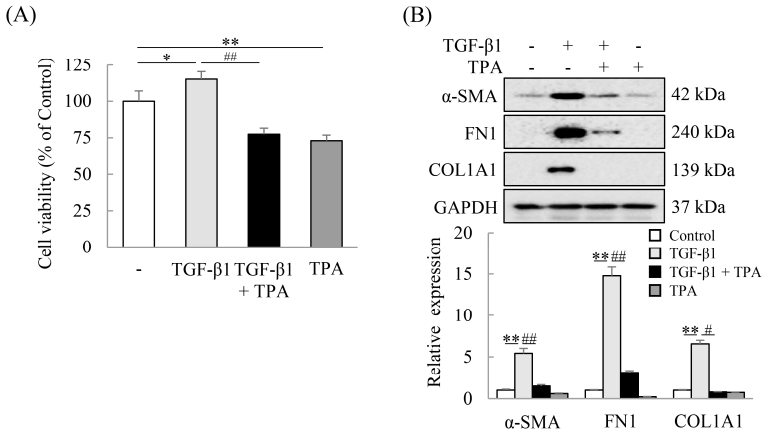

Figure 1: Decreased TGF-β-induced proliferation and fibrosis by TPA in LX-2 cells. LX-2 cells were exposed to TGF-β1 (1 μg/mL) and/or TPA (10 nM) for 2 days to assess effects on cell growth and extracellular matrix production.

(**A**) Cell viability following treatment with TGF-β1 and/or TPA in LX-2 cells. Results are shown as the mean ± SD of four independent experiments. $^{*}p < 0.05$, $^{**}p < 0.01$ vs. control group. $^{\#\#}p < 0.01$ vs. TGF-β1 group. (**B**) α-SMA, FN1, and COL1A1 expression after TGF-β1 and/or TPA treatment for 2 days in LX-2 cells. Data represent the mean ± SD of three independent experiments. $^{**}p < 0.01$ vs. control group. $^{\#}p < 0.05$, $^{\#\#}p < 0.01$ vs. TGF-β1 group. Relative expression levels were normalized to GAPDH expression.

3.2 Effects of TPA on TGF-β1 Signaling in LX-2 Cells

Next, we analyzed YAP phosphorylation and intracellular YAP distribution to determine whether TGF-β1 and/or TPA can alter YAP activity. First, TPA-induced YAP phosphorylation began at 30 min and reached a peak at 3 h, whereas AKT dephosphorylation was initiated at 15 min and sustained thereafter (Fig. A1). TGF-β1 increased the nuclear accumulation of YAP, whereas TPA significantly reduced its nuclear translocation (Fig. 2A). YAP phosphorylation decreased by approximately 22.99 ± 0.09% in TGF-β1-treated cells compared to that in controls, whereas TPA increased YAP phosphorylation by approximately two-fold relative to that in controls, irrespective of TGF-β1 treatment. Furthermore, AKT phosphorylation, one of the non-canonical TGF-β signals, was completely abolished by TPA (Fig. 2B). These results suggest that TGF-β signaling can be regulated through YAP and AKT activity, and TPA-mediated YAP and AKT regulation is crucial for suppressing hepatic stellate cell activation. We previously reported that TPA regulates YAP phosphorylation through a PKC-δ-dependent mechanism [33]. To determine whether the effects of TPA on YAP and AKT signaling, and fibrotic responses are mediated by PKC activity, LX-2 cells were treated with the pan-PKC inhibitor, Go 6983. Go 6983 markedly reduced TPA-induced YAP phosphorylation and restored AKT phosphorylation (Fig. 3A). Moreover, while TPA significantly suppressed TGF-β1-induced FN1 expression, co-treatment with Go 6983 restored the expression of these fibrotic markers to levels comparable to those observed with TGF-β1 treatment alone (Fig. 3A). Consistently, the TPA-induced reduction in cell proliferation in TGF-β1-treated LX-2 cells was also reversed by PKC inhibition (Fig. 3B). Collectively, these results indicate that TPA-induced YAP phosphorylation and AKT dephosphorylation are PKC-dependent, and PKCs activated by TPA serve as key mediators controlling proliferation and fibrotic gene expression in TGF-β1-activated hepatic stellate cells.

3.3 Role of YAP and AKT on Fibrosis in LX-2 Cells

TPA phosphorylated YAP, dephosphorylated AKT, and mitigated fibrosis in TGF-β1-treated LX-2 cells (Figs. 1 and 2); therefore, we examined whether YAP and AKT directly regulate fibrosis using specific inhibitors. First, we determined the half maximal inhibitory concentration (IC_{50}) of the YAP inhibitor, VP, and the AKT inhibitor, AKTI-1/2, on their respective targets, CYR61 and AKT. AKTI-1/2 and VP reduced AKT phosphorylation (IC_{50} = 54.79 ± 4.85 nM) and CYR61 expression (IC_{50} = 298.05 ± 12.45 nM) in a dose-dependent manner (Fig. 4). TGF-β1-induced FN1 expression decreased at concentrations above the IC_{50} of AKTI-1/2. However, even at an approximately 10-fold higher concentration (0.5 μM), AKTI-1/2 reduced FN1 by only 20.64 ± 0.07% compared to that in the control group (Fig. 5A). In contrast, VP reduced TGF-β1-induced FN1 expression starting at 250 nM, lower than its IC_{50} value (298.05 ± 12.45 nM; Fig. 5B). Furthermore, co-treatment with AKTI-1/2 and VP at their respective IC_{50} concentrations did not result in additional reduction in FN1 expression compared with VP alone (Fig. 5C). These results indicate that YAP activity, rather than AKT activity, more effectively regulates FN1 expression. Therefore, TPA simultaneously modulates canonical and non-canonical TGF-β signaling pathways through YAP phosphorylation and AKT dephosphorylation, but it modulates hepatic stellate cell fibrotic activity via YAP phosphorylation.

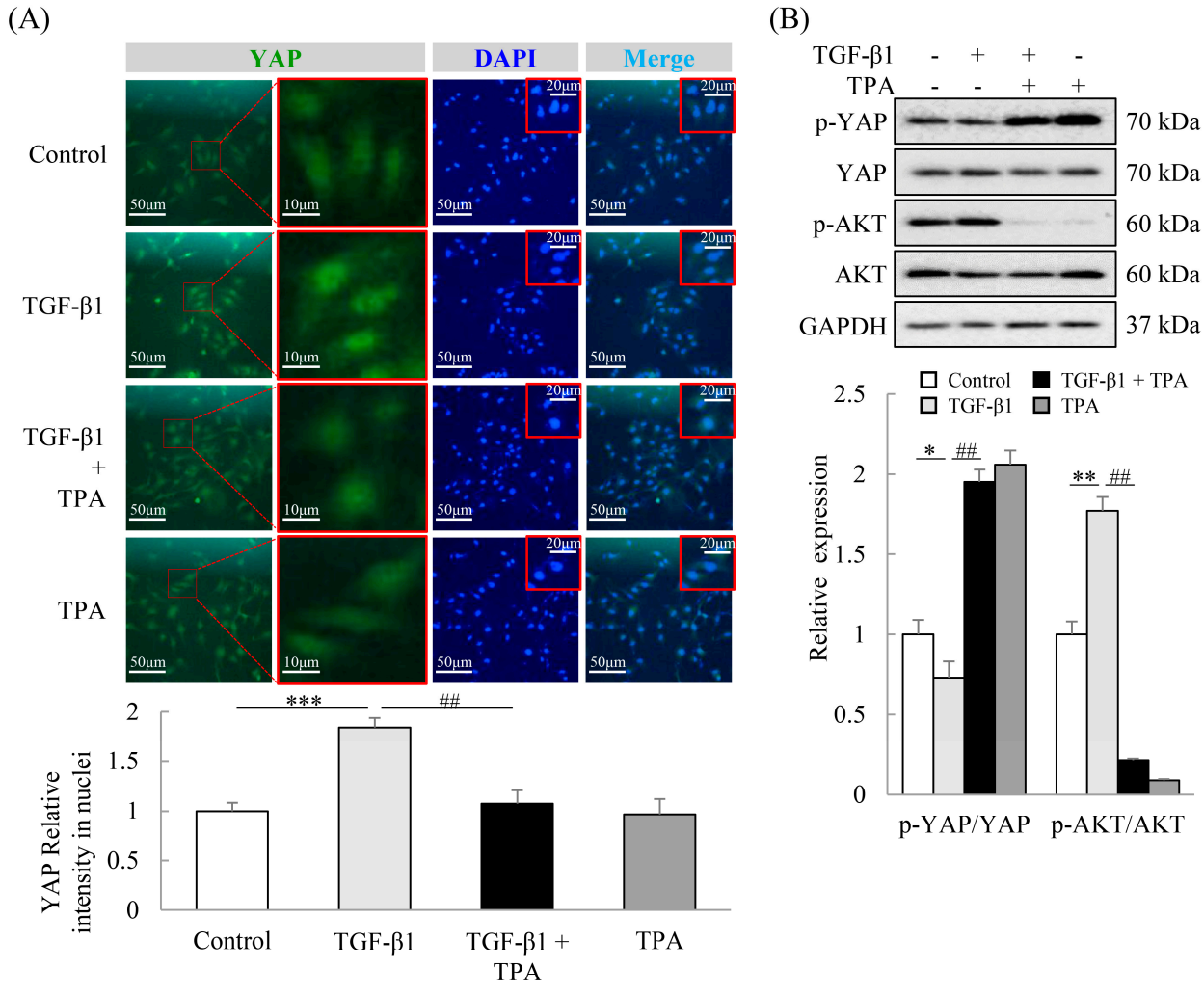

Figure 2: TPA-mediated YAP and AKT regulation in LX-2 cells. LX-2 cells were exposed to TGF-β1 (1 ng/mL), TPA (10 nM), or both agents for 3 h. YAP cellular localization and YAP and AKT phosphorylation were analyzed by immunocytochemistry and immunoblotting, respectively. (**A**) Cellular distribution of YAP in LX-2 cells. The red boxed region in the YAP immunofluorescence image on the left is magnified and shown on the right. Insets in the DAPI and merged images correspond to magnified views of the same region shown in the YAP panel. Nuclear YAP fluorescence intensity was quantified using ImageJ software. Measurements were obtained from three randomly selected fields, with more than 30 cells analyzed per field. Results are expressed as the mean ± SD of three independent experiments. $^{***}p < 0.001$ vs. control group. $^{\#\#}p < 0.01$ vs. TGF-β1 group. (**B**) Phosphorylation of AKT and YAP in LX-2 cells. Band intensities were quantified using ImageJ, and relative values were normalized to total AKT or total YAP, respectively. Data are shown as the mean ± SD of three independent experiments. $^{*}p < 0.05$, $^{**}p < 0.01$ vs. control group. $^{\#\#}p < 0.01$ vs. TGF-β1 group.

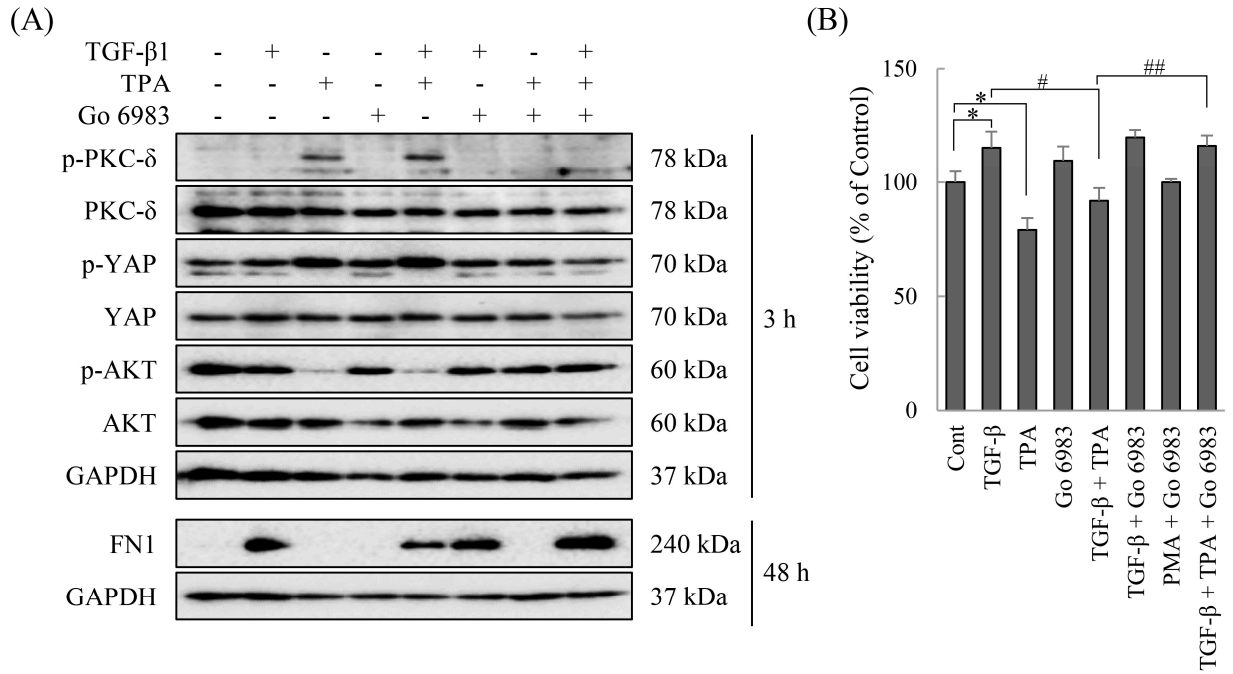

Figure 3: Fibrosis and proliferation regulation by the pan-PKC inhibitor (Go 6983) in LX-2 cells. To evaluate whether the inhibitory effects of TPA on TGF-β1-driven fibrogenic responses and proliferation are PKC-dependent, LX-2 cells stimulated with TGF-β1 were exposed to Go 6983, an inhibitor of pan-PKCs. Go 6983 reversed the inhibitory effects on fibrosis (**A**) and proliferation (**B**) observed in LX-2 cells co-treated with TGF-β1 and TPA. Data are expressed as mean ± SD of four independent experiments. $^{*}p < 0.05$ vs. control group. $^{\#}p < 0.05$, $^{\#\#}p < 0.01$ vs. TGF-β1 or TGF-β1 + TPA group.

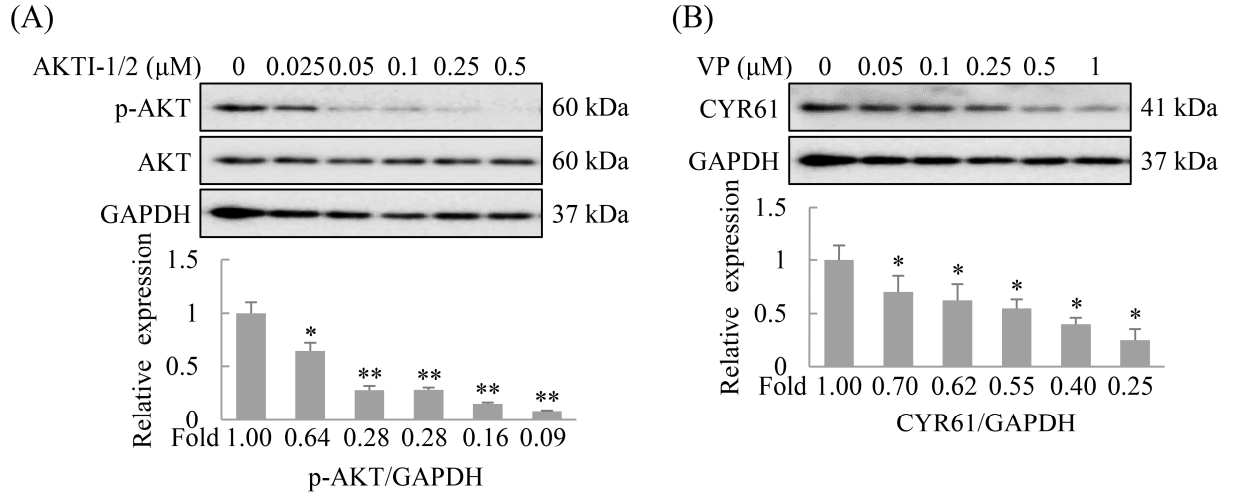

Figure 4: Inhibitory effects of AKTI-1/2 or verteporfin on AKT phosphorylation and CYR61 expression in LX-2 cells. To establish the half-maximal inhibitory concentration (IC_{50}) of AKTI-1/2 and VP for AKT phosphorylation and CYR61 expression, respectively, LX-2 cells were exposed to AKTI-1/2 or VP for 3 h. AKT phosphorylation (**A**) and CYR61 protein level (**B**) were then assessed by immunoblotting. Band intensities were quantified by densitometric analysis using ImageJ and normalized to GAPDH. Results are shown as the mean ± SD from three independent experiments. $^{*}p < 0.05$, $^{**}p < 0.01$ vs. control group.

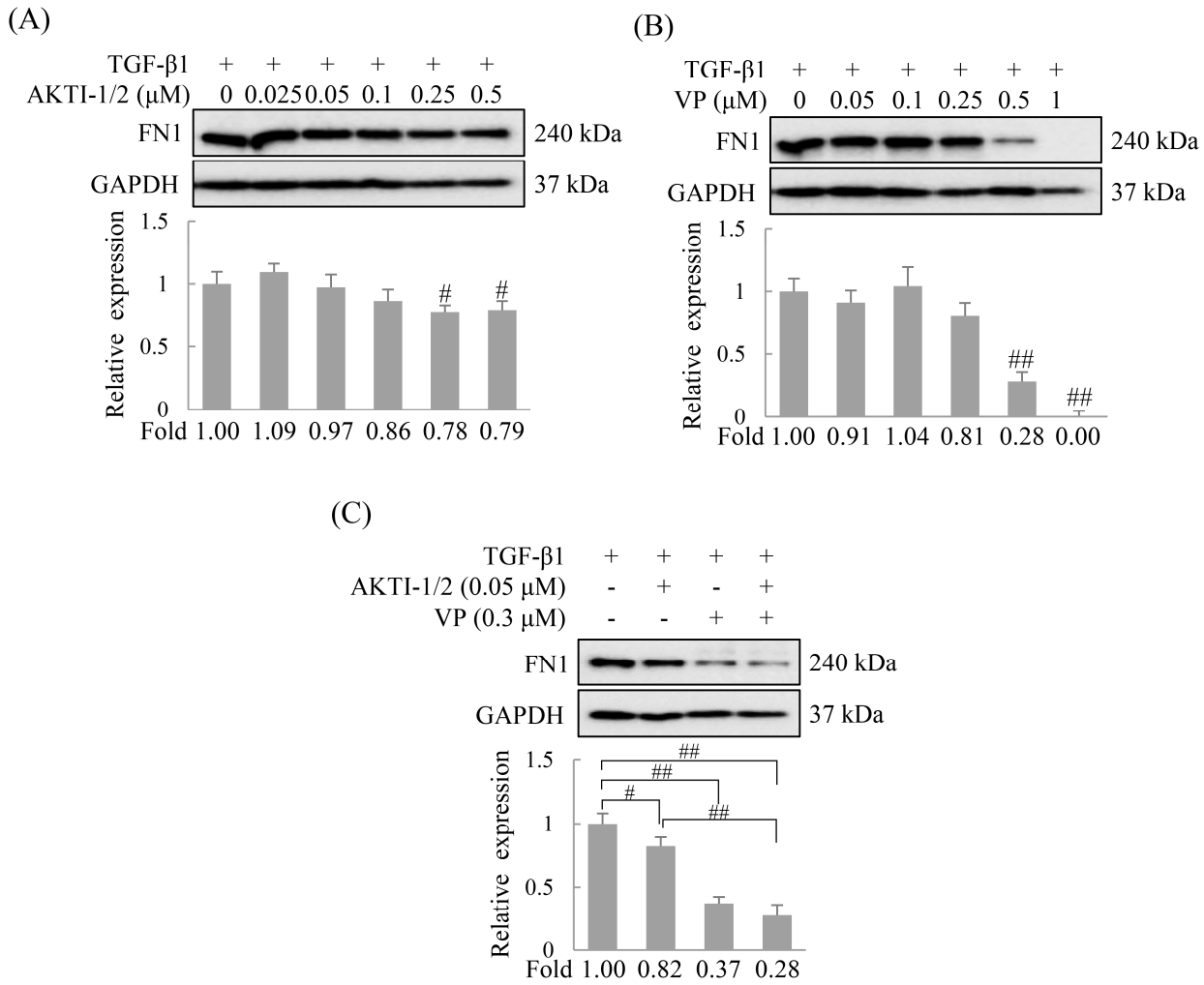

Figure 5: Role of YAP and AKT in fibrosis in LX-2 cells. To evaluate the roles of YAP and AKT in fibrosis, LX-2 cells stimulated with TGF-β1 were treated with VP or AKTI-1/2, inhibitors of YAP or AKT, respectively. (**A**) Fibrotic effect of AKT inhibition in LX-2 cells. $^{\#}p < 0.05$ vs. TGF-β1 group. (**B**) Fibrotic effect of YAP inhibition in LX-2 cells. $^{\#\#}p < 0.01$ vs. TGF-β1 group. (**C**) Cooperative fibrotic effects of YAP and AKT inhibition in TGF-β1-treated LX-2 cells. Protein band intensities were measured by densitometric analysis using ImageJ and normalized to GAPDH. Data represent the mean ± SD from three independent experiments. $^{\#}p < 0.05$, $^{\#\#}p < 0.01$ vs. TGF-β1 or TGF-β1 + AKTI-1/2 group.

3.4 Role of YAP and AKT on Proliferation of LX-2 Cells

Next, we investigated whether the modulation of YAP and AKT activity affects TGF-β1-induced LX-2 cell proliferation. Cell proliferation was analyzed following treatment of TGF-β1-exposed LX-2 cells with AKTI-1/2 and/or VP. In TGF-β1-untreated LX-2 cells, AKTI-1/2 and VP reduced proliferation at concentrations above 0.25 and 0.5 μM, respectively. However, in TGF-β1-treated LX-2 cells, no reduction in proliferation was observed (Figs. 5B and 6A). Moreover, AKTI-1/2 increased TGF-β1-induced proliferation (Fig. 6A). In contrast, synergistic inhibition of proliferation was observed when AKTI-1/2 and VP were co-administered with TGF-β1 at their respective IC_{50} concentrations (Fig. 6C). That is, AKTI-1/2 and VP individually reduced TGF-β-treated LX-2 cell proliferation by approximately 7.02 ± 0.05% and 8.98 ± 0.04%, respectively, whereas combined treatment with both inhibitors resulted in a marked synergistic reduction in proliferation of approximately 37.36 ± 0.04% (Fig. 6C). These results indicate that TGF-β-activated hepatic

stellate cells regulate proliferation via YAP and AKT, and both the canonical and non-canonical signaling pathways cooperatively modulate this process.

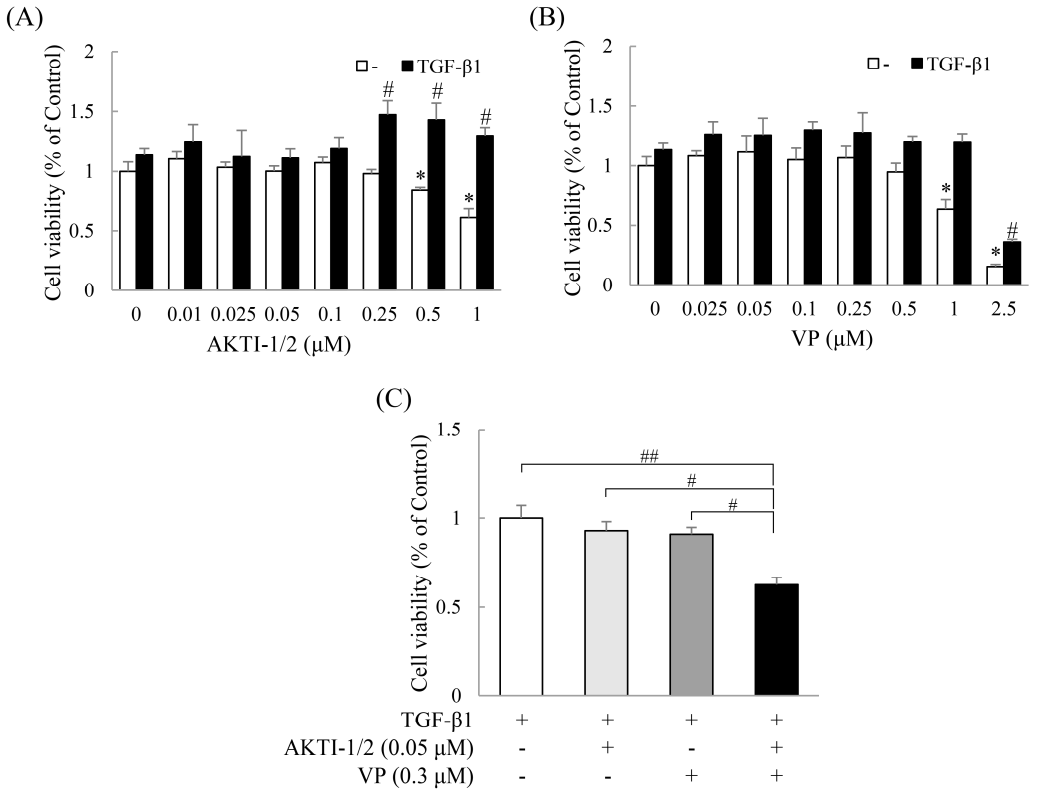

Figure 6: Role of YAP and AKT in proliferation of LX-2 cells. To evaluate the contribution of YAP and AKT to cell growth, LX-2 cells stimulated with TGF-β1 were treated with VP or AKTI-1/2, inhibitors of YAP or AKT, respectively. (**A**) AKT-mediated cell proliferation in LX-2 cells. $^{*}p < 0.05$ vs. control group. $^{\#}p < 0.05$ vs. TGF-β1 group. (**B**) YAP-mediated cell proliferation in LX-2 cells. $^{*}p < 0.05$ vs. control group. $^{\#}p < 0.05$ vs. TGF-β1 group. (**C**) Cooperative inhibition of proliferation by YAP and AKT inhibitors in TGF-β1-treated LX-2 cells. Values are expressed as the mean ± SD of four independent experiments. $^{\#}p < 0.05$ and $^{\#\#}p < 0.01$ vs. TGF-β1 or TGF-β1 + VP group.

4 Discussion

TPA increased YAP phosphorylation/AKT dephosphorylation while decreasing both proliferation and the expression of α-SMA, FN1, and COL1A1 in TGF-β1-activated LX-2 cells. Under single treatment or co-treatment with the YAP (VP) and AKT inhibitor (AKTI-1/2), the VP IC_{50} concentration significantly reduced FN1 expression in TGF-β1-treated LX-2 cells; however, no synergistic reduction in FN1 expression was observed under co-treatment conditions at the IC_{50} concentration. Co-administration of both inhibitors significantly reduced proliferation in TGF-β1-treated LX-2 cells, despite neither inhibitor alone significantly reducing cell proliferation at their IC_{50} concentrations. These results suggest that while canonical TGF-β signaling primarily regulates fibrosis, both canonical and non-canonical TGF-β signaling pathways synergistically regulate hepatic stellate cell proliferation more effectively. Although our data suggest that modulation of YAP- and AKT-associated pathways differentially affects fibrotic marker expression and proliferative responses in LX-2 cells, the precise mechanistic relationship between these pathways remains unclear. Therefore, their roles should be interpreted as functionally associated rather than independently or cooperatively validated at the mechanistic level. Further studies will be required to determine how

these pathways interact to regulate fibrosis and proliferation. The non-canonical TGF-β signaling pathway is mediated by Rho, MAPK, and/or AKT, acting either independently or in coordination with SMADs to regulate downstream responses [3,8,13]. Among them, AKT can be activated by TGF-β through PI3K [40], TRAF6 [41], microRNAs such as miR-216a/217 and miR-21 [42,43], or TGF-α expression [44]. TGF-β-AKT signaling regulates epithelial-to-mesenchymal transition, SMAD-mediated transcription, and fibroblast proliferation [45–47]. In this study, AKTI-1/2 partially inhibited TGF-β1-induced FN1 expression even at concentrations approximately 10-fold higher than its IC_{50}, but did not inhibit TGF-β1-induced proliferation. This suggests that AKT alone is insufficient to regulate hepatic stellate cell proliferation and fibrosis. Conversely, VP effectively reduced TGF-β-induced FN1 expression at its IC_{50} concentration but did not inhibit TGF-β-induced proliferation. These results indicate that although both canonical and non-canonical signaling pathways can regulate fibrosis, the canonical pathway is a more efficient regulator, and cooperation between the two is required for hepatic stellate cell proliferation.

A limitation of this study is that the interaction between YAP and SMAD was not directly examined. In addition to serving as transcriptional cofactors that promote TGF-β signaling [48,49], YAP/TAZ regulate fibrosis by influencing SMAD nucleocytoplasmic shuttling [50,51], maintaining nuclear retention of activated SMAD2/3 [51,52], and acting as mechanoregulators of TGF-β-SMAD signaling [52]. Thus, it is important to determine how the individual activities of YAP and SMAD regulate fibrosis in TGF-β-activated hepatic stellate cells. Our future studies will use RNA interference experiments to selectively modulate YAP and SMAD expression and analyze the effects on fibrosis. Furthermore, validation in experimental models of fibrosis will be required to assess the antifibrotic potential of targeting canonical and non-canonical TGF-β signaling pathways, either separately or in combination. Although the present study demonstrates that TPA modulates YAP- and AKT-associated signaling and attenuates TGF-β1-induced responses in hepatic stellate cells, it does not fully elucidate the underlying molecular mechanisms. Therefore, the therapeutic implications of TPA in fibrosis should be interpreted with caution. Further mechanistic studies, as well as *in vivo* validation, will be required to determine whether targeting these pathways can be translated into effective anti-fibrotic strategies. TPA promotes and inhibits proliferation or fibrosis in a cell-type-dependent manner; however, its clinical application remains challenging. Additional investigations are needed to determine whether targeting canonical and non-canonical TGF-β signaling pathways, either individually or in combination, can be effectively developed as therapeutic strategies for fibrotic disorders.

5 Conclusion

TGF-β1 stimulation enhanced LX-2 cell growth and upregulated fibrotic markers, including α-SMA, FN1, and COL1A1. However, TPA reduced both proliferation and fibrotic protein expression in TGF-β1-activated LX-2 cells. This effect occurred because TPA induced YAP phosphorylation and AKT dephosphorylation, thereby inhibiting the activities of both YAP and AKT. YAP activity regulated fibrotic protein expression in LX-2 cells; however, in TGF-β1-activated LX-2 cells, simultaneously inhibiting both YAP and AKT was more effective at suppressing proliferation. These results suggest that coordinated regulation of YAP and AKT activity is essential for controlling fibroblast proliferation and ECM production. Moreover, TPA, which modulates both YAP and AKT activity, may represent a promising therapeutic candidate for liver fibrosis.

Acknowledgement: Not applicable.

Funding Statement: This research was funded by the Basic Science Research Program through the National Research Foundation of Korea (NRF), grant numbers RS-2023-00250982 and 2021R1I1A1A01056265.

Author Contributions: The authors confirm contribution to the paper as follows: Conceptualization, Moo Hyun Kim, Yongdae Yoon, Chang Wan Kim, Pil Young Jung, Young Woo Eom; formal analysis, Moo Hyun Kim; Investigation, Moo Hyun Kim, Yongdae Yoon, Chang Wan Kim, Jun-Won Lee, Bhupendra Regmi, Saher Fatima, Moon Young Kim, Soon Koo Baik; writing—original draft preparation, Young Woo Eom; writing—review and editing, Moo Hyun Kim, Bhupendra Regmi, Supervision, Pil Young Jung, Young Woo Eom; funding acquisition, Pil Young Jung, Young Woo Eom. All authors reviewed and approved the final version of the manuscript.

Availability of Data and Materials: The data that support the findings of this study are available from the corresponding authors upon reasonable request.

Ethics Approval: Not applicable.

Conflicts of Interest: The authors declare no conflicts of interest.

Abbreviations

α-SMA	α-Smooth muscle actin
ECM	Extracellular matrix
FN1	Fibronectin
IC_{50}	Half maximal inhibitory concentration
MAPK	Mitogen-activated protein kinase
PI3K	Phosphatidylinositol 3-kinase
AKT	Protein kinase B
PKC	Protein kinase C
TGF-β	Transforming growth factor beta
TPA	2-O-tetradecanoylphorbol-13-acetate
TAZ	Transcriptional coactivator with PDZ-binding motif
TEAD	Transcriptional enhancer activator domain
VP	Verteporfin, VP
YAP	Yes-associated protein

Appendix A

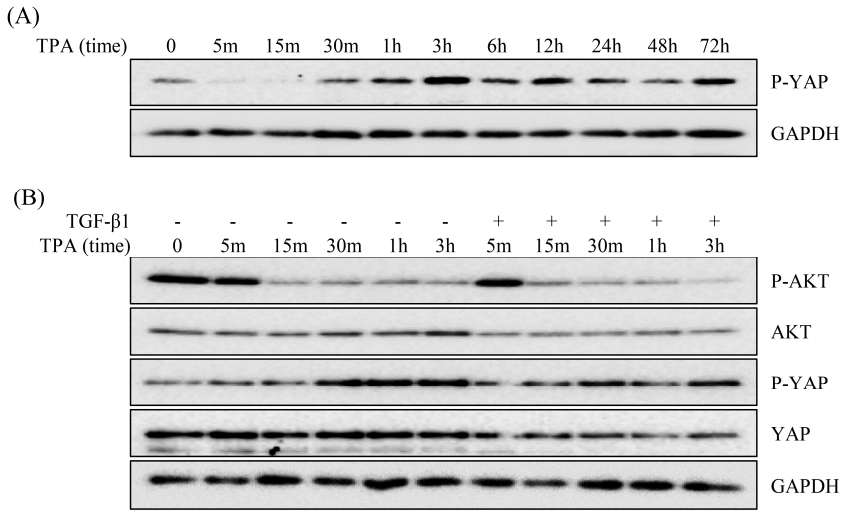

Figure A1: TPA-induced YAP phosphorylation and AKT dephosphorylation over time. LX-2 cells were treated with TPA and phosphorylation was analyzed using immunoblotting. YAP phosphorylation began at 30 minutes and was maintained for up to 3 days, reaching a peak at 3 h (**A**). In LX-2 cells exposed to TPA or TGF-β + TPA, AKT was dephosphorylated starting at 15 min and up to 3 h (**B**).

References

1. Derynck R, Akhurst RJ. Differentiation plasticity regulated by TGF-beta family proteins in development and disease. Nat Cell Biol. 2007;9(9):1000–4. [CrossRef].
2. Massagué J, Seoane J, Wotton D. Smad transcription factors. Genes Dev. 2005;19(23):2783–810. [CrossRef].
3. Moustakas A, Heldin CH. The regulation of TGFbeta signal transduction. Development. 2009;136(22):3699–714. [CrossRef].
4. Bhardwaj S, Gautam RK, Kushwaha S. From senescence to scarring: exploring TGF-β signaling in cellular aging, fibrotic remodeling, and pulmonary fibrosis. Cytokine Growth Factor Rev. 2025;86:29–39. [CrossRef].
5. Chen Y, Yuan S, Cao Y, Kong G, Jiang F, Li Y, et al. Gasotransmitters: potential therapeutic molecules of fibrotic diseases. Oxid Med Cell Longev. 2021;2021:3206982. [CrossRef].
6. Yoshida K, Matsuzaki K. Differential regulation of TGF-β/smad signaling in hepatic stellate cells between acute and chronic liver injuries. Front Physio. 2012;3:53. [CrossRef].
7. Dewidar B, Meyer C, Dooley S, Meindl-Beinker AN. TGF-β in hepatic stellate cell activation and liver fibrogenesis-updated 2019. Cells. 2019;8(11):1419. [CrossRef].
8. Finnson KW, Almadani Y, Philip A. Non-canonical (non-SMAD2/3) TGF-β signaling in fibrosis: mechanisms and targets. Semin Cell Dev Biol. 2020;101:115–22. [CrossRef].
9. Shi Y, Massagué J. Mechanisms of TGF-beta signaling from cell membrane to the nucleus. Cell. 2003;113(6):685–700. [CrossRef].
10. Chaudhary R, Weiskirchen R, Ehrlich M, Henis YI. Dual signaling pathways of TGF-β superfamily cytokines in hepatocytes: balancing liver homeostasis and disease progression. Front Pharmacol. 2025;16:1580500. [CrossRef].
11. Fabregat I, Moreno-Càceres J, Sánchez A, Dooley S, Dewidar B, Giannelli G, et al. TGF-β signalling and liver disease. FEBS J. 2016;283(12):2219–32. [CrossRef].
12. Zargar AM, Ali Z, Fallah A, Mohagheghi S. TGF-β/Smad signaling pathway in fatty liver disease: a case-control study. Mol Biol Rep. 2024;51(1):1031. [CrossRef].
13. Hong M, Wilkes MC, Penheiter SG, Gupta SK, Edens M, Leof EB. Non-Smad transforming growth factor-β signaling regulated by focal adhesion kinase binding the p85 subunit of phosphatidylinositol 3-kinase. J Biol Chem. 2011;286(20):17841–50. [CrossRef].
14. Link PA, Choi KM, Diaz Espinosa AM, Jones DL, Gao AY, Haak AJ, et al. Combined control of the fibroblast contractile program by YAP and TAZ. Am J Physiol Lung Cell Mol Physiol. 2022;322(1):L23–32. [CrossRef].
15. Liu F, Lagares D, Choi KM, Stopfer L, Marinković A, Vrbanac V, et al. Mechanosignaling through YAP and TAZ drives fibroblast activation and fibrosis. Am J Physiol Lung Cell Mol Physiol. 2015;308(4):L344–57. [CrossRef].
16. Francisco J, Zhang Y, Jeong JI, Mizushima W, Ikeda S, Ivessa A, et al. Blockade of fibroblast YAP attenuates cardiac fibrosis and dysfunction through MRTF-a inhibition. JACC Basic Transl Sci. 2020;5(9):931–45. [CrossRef].
17. Mia MM, Cibi DM, Ghani SABA, Singh A, Tee N, Sivakumar V, et al. Loss of Yap/Taz in cardiac fibroblasts attenuates adverse remodelling and improves cardiac function. Cardiovasc Res. 2022;118(7):1785–804. [CrossRef].
18. Zhou Y, Liang P, Bi T, Tang B, Zhu X, Liu X, et al. Angiotensin II depends on hippo/YAP signaling to reprogram angiogenesis and promote liver fibrosis. Cell Signal. 2024;123:111355. [CrossRef].
19. Li C, Zhang R, Zhan Y, Zheng J. Resveratrol inhibits hepatic stellate cell activation via the hippo pathway. Mediators Inflamm. 2021;2021:3399357. [CrossRef].
20. Gui Y, Li J, Lu Q, Feng Y, Wang M, He W, et al. Yap/Ta_z mediates mTORC2-stimulated fibroblast activation and kidney fibrosis. J Biol Chem. 2018;293(42):16364–75. [CrossRef].
21. Habshi T, Shelke V, Kale A, Lech M, Gaikwad AB. Hippo signaling in acute kidney injury to chronic kidney disease transition: current understandings and future targets. Drug Discov Today. 2023;28(8):103649. [CrossRef].
22. Piersma B, de Rond S, Werker PMN, Boo S, Hinz B, van Beuge MM, et al. YAP1 is a driver of myofibroblast differentiation in normal and diseased fibroblasts. Am J Pathol. 2015;185(12):3326–37. [CrossRef].
23. Ledwon JK, Progri B, Applebaum SA, Vignesh O, Yau A, Aguilar AH, et al. Hippo pathway regulates cell proliferation in skin epidermis exposed to mechanical forces. J Cell Mol Med. 2025;29(12):e70674. [CrossRef].
24. Callus BA, Finch-Edmondson ML, Fletcher S, Wilton SD. YAPping about and not forgetting TAZ. FEBS Lett. 2019;593(3):253–76. [CrossRef].

25. Heng BC, Zhang X, Aubel D, Bai Y, Li X, Wei Y, et al. An overview of signaling pathways regulating YAP/TAZ activity. Cell Mol Life Sci. 2021;78(2):497–512. [CrossRef].
26. Noorbakhsh N, Hayatmoghadam B, Jamali M, Golmohammadi M, Kavianpour M. The Hippo signaling pathway in leukemia: function, interaction, and carcinogenesis. Cancer Cell Int. 2021;21(1):705. [CrossRef].
27. Boopathy GTK, Hong W. Role of hippo pathway-YAP/TAZ signaling in angiogenesis. Front Cell Dev Biol. 2019;7:49. [CrossRef].
28. Mia MM, Singh MK. New insights into hippo/YAP signaling in fibrotic diseases. Cells. 2022;11(13):2065. [CrossRef].
29. Zhang K, Chang Y, Shi Z, Han X, Han Y, Yao Q, et al. ω-3 PUFAs ameliorate liver fibrosis and inhibit hepatic stellate cells proliferation and activation by promoting YAP/TAZ degradation. Sci Rep. 2016;6:30029. [CrossRef].
30. Baldan S, Meriin AB, Yaglom J, Alexandrov I, Varelas X, Xiao ZJ, et al. The Hsp70-Bag3 complex modulates the phosphorylation and nuclear translocation of Hippo pathway protein Yap. J Cell Sci. 2021;134(23):jcs259107. [CrossRef].
31. Gallardo FS, Cruz-Soca M, Bock-Pereda A, Faundez-Contreras J, Gutiérrez-Rojas C, Gandin A, et al. Role of TGF-β/SMAD/YAP/TAZ signaling in skeletal muscle fibrosis. Am J Physiol Cell Physiol. 2025;328(3):C1015–28. [CrossRef].
32. Futakuchi A, Inoue T, Wei FY, Inoue-Mochita M, Fujimoto T, Tomizawa K, et al. YAP/TAZ are essential for TGF-β2-mediated conjunctival fibrosis. Investig Ophthalmol Vis Sci. 2018;59(7):3069–78. [CrossRef].
33. Kim CW, Yoon Y, Kim MY, Baik SK, Ryu H, Park IH, et al. 12-O-tetradecanoylphorbol-13-acetate reduces activation of hepatic stellate cells by inhibiting the hippo pathway transcriptional coactivator YAP. Cells. 2022;12(1):91. [CrossRef].
34. Ji D, Zhao Q, Qin Y, Tong H, Wang Q, Yu M, et al. Germacrone improves liver fibrosis by regulating the PI3K/AKT/mTOR signalling pathway. Cell Biol Int. 2021;45(9):1866–75. [CrossRef].
35. Wu L, Zhang Q, Mo W, Feng J, Li S, Li J, et al. Quercetin prevents hepatic fibrosis by inhibiting hepatic stellate cell activation and reducing autophagy via the TGF-β1/Smads and PI3K/Akt pathways. Sci Rep. 2017;7:9289. [CrossRef].
36. Wang R, Song F, Li S, Wu B, Gu Y, Yuan Y. Salvianolic acid A attenuates CCl_4-induced liver fibrosis by regulating the PI3K/AKT/mTOR, Bcl-2/Bax and caspase-3/cleaved caspase-3 signaling pathways. Drug Des Dev Ther. 2019;13:1889–900. [CrossRef].
37. Ragolia L, Palaia T, Paric E, Maesaka JK. Elevated L-PGDS activity contributes to PMA-induced apoptosis concomitant with downregulation of PI3-K. Am J Physiol Cell Physiol. 2003;284(1):C119–26. [CrossRef].
38. Zheng WH, Kar S, Quirion R. Stimulation of protein kinase C modulates insulin-like growth factor-1-induced Akt activation in PC12 cells. J Biol Chem. 2000;275(18):13377–85. [CrossRef].
39. Razmara M, Heldin CH, Lennartsson J. Platelet-derived growth factor-induced Akt phosphorylation requires mTOR/Rictor and phospholipase C-γ1, whereas S6 phosphorylation depends on mTOR/Raptor and phospholipase D. Cell Commun Signal. 2013;11(1):3. [CrossRef].
40. Cheng WC, Chen PY, Zhang X, Chang YK, Tan KT, Lin TCC. 5,7,3′,4′-Tetramethoxyflavone suppresses TGF-β1-induced activation of murine fibroblasts *in vitro* and ameliorates bleomycin-induced pulmonary fibrosis in mice. Immunopharmacol Immunotoxicol. 2024;46(4):496–508. [CrossRef].
41. Yang WL, Wang J, Chan CH, Lee SW, Campos AD, Lamothe B, et al. The E3 ligase TRAF6 regulates Akt ubiquitination and activation. Science. 2009;325(5944):1134–8. [CrossRef].
42. Dey N, Ghosh-Choudhury N, Kasinath BS, Choudhury GG. TGFβ-stimulated microRNA-21 utilizes PTEN to orchestrate AKT/mTORC1 signaling for mesangial cell hypertrophy and matrix expansion. PLoS One. 2012;7(8):e42316. [CrossRef].
43. Kato M, Putta S, Wang M, Yuan H, Lanting L, Nair I, et al. TGF-beta activates Akt kinase through a microRNA-dependent amplifying circuit targeting PTEN. Nat Cell Biol. 2009;11(7):881–9. [CrossRef].
44. Viñals F, Pouysségur J. Transforming growth factor beta1 (TGF-beta1) promotes endothelial cell survival during *in vitro* angiogenesis via an autocrine mechanism implicating TGF-alpha signaling. Mol Cell Biol. 2001;21(21):7218–30. [CrossRef].
45. Julien S, Puig I, Caretti E, Bonaventure J, Nelles L, van Roy F, et al. Activation of NF-kappaB by Akt upregulates Snail expression and induces epithelium mesenchyme transition. Oncogene. 2007;26(53):7445–56. [CrossRef].

46. Conery AR, Cao Y, Thompson EA, Townsend CM, Ko TC, Luo K. Akt interacts directly with Smad3 to regulate the sensitivity to TGF-β-induced apoptosis. Nat Cell Biol. 2004;6(4):366–72. [CrossRef].
47. Wilkes MC, Mitchell H, Penheiter SG, Doré JJ, Suzuki K, Edens M, et al. Transforming growth factor-beta activation of phosphatidylinositol 3-kinase is independent of Smad2 and Smad3 and regulates fibroblast responses via p21-activated kinase-2. Cancer Res. 2005;65(22):10431–40. [CrossRef].
48. Grannas K, Arngården L, Lönn P, Mazurkiewicz M, Blokzijl A, Zieba A, et al. Crosstalk between hippo and TGFβ: subcellular localization of YAP/TAZ/smad complexes. J Mol Biol. 2015;427(21):3407–15. [CrossRef].
49. Savorani C, Malinverno M, Seccia R, Maderna C, Giannotta M, Terreran L, et al. A dual role of YAP in driving TGFβ-mediated endothelial-to-mesenchymal transition. J Cell Sci. 2021;134(15):jcs251371. [CrossRef].
50. Beyer TA, Weiss A, Khomchuk Y, Huang K, Ogunjimi AA, Varelas X, et al. Switch enhancers interpret TGF-β and Hippo signaling to control cell fate in human embryonic stem cells. Cell Rep. 2013;5(6):1611–24. [CrossRef].
51. Varelas X, Sakuma R, Samavarchi-Tehrani P, Peerani R, Rao BM, Dembowy J, et al. TAZ controls Smad nucleocytoplasmic shuttling and regulates human embryonic stem-cell self-renewal. Nat Cell Biol. 2008;10(7):837–48. [CrossRef].
52. Szeto SG, Narimatsu M, Lu M, He X, Sidiqi AM, Tolosa MF, et al. YAP/TAZ are mechanoregulators of TGF-β-smad signaling and renal fibrogenesis. J Am Soc Nephrol. 2016;27(10):3117–28. [CrossRef].